Preliminary Studies on the Characteristics of the Induced Currents in Simple Down Conductors Due to a Nearby Lightning Strike

Udaya Kumar, Vishwanath Hegde, and Vinoda Shivanand

***Abstract*—A lightning strike in a neighborhood can induce significant currents in tall down conductors. Although the magnitude of current in this case is much smaller than that encountered during a direct strike, the probability of occurrence and the frequency content is higher. In view of this, appropriate knowledge of the characteristics of such induced currents is relevant for the scrutinization of the recorded currents. Considering these, the present paper makes a preliminary investigation into the basic characteristics of lightning-induced currents in simple tall vertical down conductors. The electromagnetic model is employed for the study, and NEC-2 is employed for the numerical field computations. Laboratory experiments with reduced-scale electromagnetic model of the system are employed to validate the numerical approach. The influence of important parameters has been investigated and highly insightful results obtained. The induced current is found to depend on the maximum rate of rise of the stroke current and its velocity of propagation, the height of the down conductor, and the footing impedance. The channel inclination and the distance between the channel and the down conductor have significant influence on the magnitude of the induced current. It is found that the radius of the down conductor is not very influential. The induced current due to a stroke on a nearby conducting object of considerable height can have different overall features.**

***Index Terms*—Down conductors and towers, induced currents, lightning, lightning-induced surges.**

I. Introduction

A lightning strike in the neighborhood can induce appreciable currents in the down conductors. The magnitudes of such induced currents are definitely lower than those encountered during a direct hit. However, their frequency of occurrence is comparatively higher. Appropriate knowledge of the characteristics of the induced currents would help in the characterization and classification of the recorded currents on instrumented down conductors. Such knowledge would also be useful for the study of the electromagnetic noise/disturbances caused by the induced currents on the electrical and electronic system in the vicinity and for the system mounted on the down conductors (towers). For a rough estimation of the number of strikes in the surrounding area, the information on the annual frequency of induction due to a strike in the vicinity can be used in conjunction with the number of direct hits. In view of these facts, investigations on the characteristics of the induced currents seem to be essential.

There is a large amount of literature on the problem of induced currents in conductors of electrical distribution lines and telecommunication lines. For example, see [1] and [2] for details. Detailed studies on the lightning-induced disturbances in buried electrical cables have also been carried out [3], [4]. Similarly, induction in the protection system as well as the electrical network of a building has also drawn attention [5], [6]. However, to the best of the author's knowledge, open literature on the characteristics of induced currents on down conductors seems to be rather limited. In view of this, a study on simple down conductors is taken up here. The present paper evaluates the basic characteristics of the induced currents in simple vertical down conductors due to a lightning strike in the vicinity.

II. Present Work

In this paper, the down conductor is modeled only as a vertical conductor. Such models have been successfully employed in the literature pertaining to the evaluation of the induced current and field due to a strike on an elevated object [7], [8]. As only the strikes that occur in the vicinity, i.e., well within a 1-km radius of the down conductor, are of interest, the ground is assumed to be perfectly conducting. Tall down conductors are known to initiate significant upward leader activities. There will be the deposition of a charge of opposite polarity on the down conductors as well as on the connecting leaders. Once the strike is complete on a remote earth/earthed object, these accumulated charges will also initiate a current in the down conductor. In this preliminary study, these effects are not considered. However, if the flash is not very close to the down conductor, the above current can be neglected. However, while applying the deductions of the present paper, the above assumptions need to be kept in mind. However, for the above-mentioned aspect, the present paper can be considered as a detailed one. Further, the other objects are assumed to be quite distant to not disturb the induced current in the down conductor under consideration.

A. Numerical Modeling Employed for the Problem

As the electromagnetic field produced by the lightning is basically responsible for the current induction, the model to be employed for the study must be based on an electromagnetic model. Such a model, which is also called the antenna theory (AT) model, has been quite successfully employed in the literature for the estimation of currents and the field in the

Manuscript received November 12, 2005; revised June 20, 2006. The work of V. Hegde and V. Shivanand was supported by the All India Council for Technical Education.

The authors are with the Department of High Voltage Engineering, Indian Institute of Science, Bangalore 560012, India (e-mail: uday@hve.iisc.ernet.in; hegde@hve.iisc.ernet.in; vinoda_shivanand@yahoo.co.in).

Digital Object Identifier 10.1109/TEMC.2006.882838

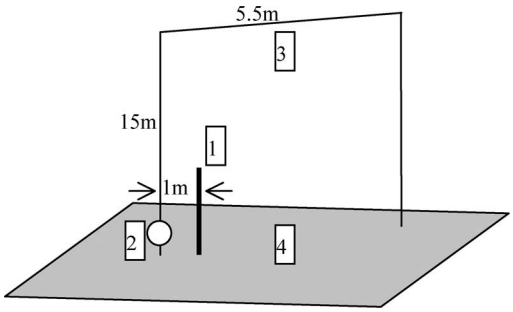

Fig. 1. Schematic of the experimental setup. (1) Down conductor (height = 3.4 m). (2) Source. (3) Current lead (channel). (4) Ground plane.

vicinity [7]–[9]. Based on this, the present paper employs an electromagnetic model, which ensures reliable description of the associated field problem. It may be noted here that the reaction field due to the currents in the down conductor, depending on its height, can be dominated by transverse magnetic modes. NEC-2 [10] is used for the required field computations, wherein the calculations are carried out in the frequency domain. Accordingly, the down conductor and the channel are modeled as cylindrical conductors. The length of the channel is selected such that the reflection originating from the top end of the channel model does not reach within the period of observation. Depending on the height of the down conductor and the distance between the channel and the down conductor, the height of the channel is selected in the range of 1–5 km. In order to respect both the upper and the lower frequency constraints on the permissible discretization length [10], a segment length of 6 m has been selected for whole of the problem. The down conductor is terminated with appropriate ground termination resistance. For realizing a reduced velocity of $c/3$ (where c is the velocity of light in free space), a uniform loading of 9-μH/m inductance and 1.0-Ω/m resistance is employed. The source modeling is the same as that adopted earlier [7]. Basically, a voltage source with a high resistance of 5 kΩ is employed. This is essential for fixing the current wave shape, especially for the strokes with current velocity close to that of light. Otherwise, a two-step procedure would become necessary, where, in the first step, the required source voltage shape is deduced for driving the required current waveform [11]. Typically, the frequency sweep for the NEC runs are selected in the range of 50 kHz to 5 MHz. The number of frequency steps is selected in the range of 512–1024. More specifically, 1024 frequency steps would be necessary for studies with tall down conductors such as CN Tower, and 512 steps are adequate for the down conductors of height shorter than or in the range of 120 m. The source waveform is modeled in a larger window with an initial and final zero padding. The zero padding is very useful in eliminating the offset and low-frequency problems that are encountered in many cases. The time-domain quantities are computed in MATLAB using appropriate Fourier techniques. The time step selected for the inversion is in the range of 25–61 ns.

B. Details of the Experimental Setup and the Results

In order to scrutinize the accuracy of the numerical model, laboratory experiments with 40:1 reduced scale models are carried out. Fig. 1 gives the schematic of the experimental setup. The basic experimental setup is the same as that given in [12]. Interconnected aluminum sheets of 0.81-mm thickness form the ground plane. The current lead is formed by a 7/20 standard (which corresponds to a 2.44-mm diameter) plastic-insulated wire gauge extended in the form of an inverted U. It extends vertically to about 15 m, which is followed by a horizontal extension of about 5.5 m. Finally, it comes vertically down along the wall (column) to meet the ground plane. A 3-mm-diameter copper rod of 3.4-m height represents the down conductor. A ground terminating resistance of 6 Ω is employed. An arbitrary waveform generator (Model 33250A; Agilent) is employed as the source. Current-to-voltage converters (Model 2877; Pearson), with 2-ns rise time, 200-MHz bandwidth, and 50-Ω output impedance are used for the noninvasive measurement of various currents. These current monitors are connected to the oscilloscope with 1-m-long Tektronix probes. The Tektronix Model TPS2024 four-channel digital storage oscilloscope is employed for measurements. It has floating channels with 200-MHz bandwidth, 2-GS/s sampling rate, and 8-bit resolution.

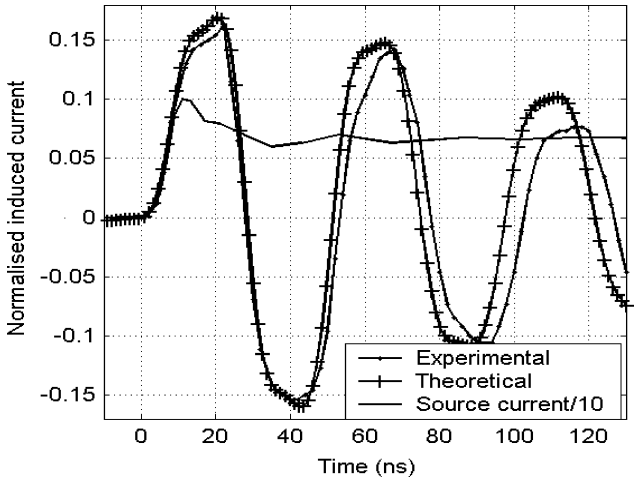

Fig. 2. Comparison of the experimentally and theoretically determined induced current waveforms.

Using the waveform generator, a repetitive pulse excitation is imposed on the current lead wire. The resulting current, as shown in Fig. 2, had a time to peak of 10 ns and a tail time of 250 ns. In order to fit into the scale, the source current is reduced by a factor of 10. The corresponding induced current waveform is also shown in Fig. 2. Using a fast pulse, the velocity of propagation on insulated copper wire representing the current lead wire is found to be close to $0.9c$ (where c is the velocity of light in free space), and the first reflection occurring at the wall junction reaches the source at about 151 ns. In the simulation, the reduced velocity is realized by a uniform loading of the channel with 0.5-Ω/m resistance and 0.5-μH/m inductance. It is evident from Fig. 2 that the comparison between the experimental and numerical results is quite satisfactory. The difference between the experimental and the theoretical waveforms seems to increase with time especially for the oscillation period. However, it must be noted that the experimental ground is not perfect, and the terminating resistance is not free of stray inductance and capacitances.

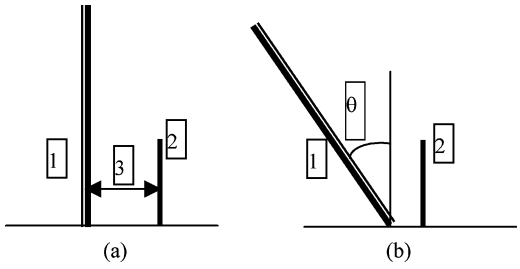

Fig. 3. Schematic layout of the channel and the down conductor. (a) Vertical channel. (b) Inclined channel. (1) Channel. (2) Downconductor. (3) Gap between the channel and the down conductor. θ is the angle of inclination of the channel with respect to the vertical.

C. Parameters for the Study

For the present paper, only the basic influential parameters are considered. With regard to the channel, the following are considered: 1) strike to the ground and a strike to an elevated strike object (ESO); 2) rate of rise of the stroke current [which for a given wave shape is related to the time to peak $(t_{\rm p})$]; 3) velocity of propagation of the stroke current (v); 4) distance of the channel from the down conductor (D); and 5) inclination of the channel with respect to the vertical. For the down conductor, the following are the basic parameters: 1) height (H); 2) radius (r)/cross section; and 3) footing resistance. For the velocity, c is taken as the upper limit and $c/3$ as the lower limit. The schematic of the problem geometry is shown in Fig. 3. Fig. 3(a) provides the schematic of the conductor and the channel. The inclination, as shown in Fig. 3(b), is always considered to be away from the down conductor. The radius employed for the lightning channel in the model, when varied in the range of 2.5 mm to 11.5 cm [13], did not show any significant influence on the computed results.

III. Simulation Results and Analyses

Under the conditions stated in Section II, the phenomena of induction to the down conductor can be treated as linear. In other words, for a given set of conditions and lightning stroke current waveform, the amplitude of the induced current varies linearly with the amplitude of the stroke current. In view of this, the stroke current is normalized to a unit amplitude.

In the first round of simulations, the stroke current is expressed by double exponential function of the form $I = I_0(e^{-at} - e^{-bt})$. Similar to the commonly employed channel base current waveform for the simulation of lightning return stroke fields [14], this waveform has the maximum *di*/*dt* region near the origin. Therefore, the influence of tail portion is segregated from that of the region in front, which produces maximum induction.

First the stroke directly terminating on the ground is considered. Unless otherwise specified, the lightning channel is assumed to be vertical, and a double exponential current of unit amplitude and a time to peak of 1.2 μs is chosen. The associated rise time between 10% and 90% is 0.565 μs. The corresponding parameters of the exponential function are $a = 3.08 \times 10^6$, $b = 6.25 \times 10^4$, and $I_0 = 1.1365$. It has been verified that the details of the slowly varying tail portion are not important. The polarity of the first swing of the induced current is always opposite from that of the stroke current. However, for plotting waveforms, the first swing is taken as positive. For normalization of the results, the induced currents are calculated for channel base current with a unit peak amplitude. Although many simulations have been carried out for different down conductor heights [15], more emphasis is given to the 120-m-tall down conductor. The default dimensions of the down conductors are height $= 120$ m and radius $= 3.8$ cm. These dimensions are selected from a system on which some instrumentation is being planned.

In the numerical procedure, an improper frequency-to-time-domain conversion can lead to a nonphysical oscillation as well as an offset extending to well before time zero, i.e., the initiation of stroke. In order to demonstrate the adequacy of the computed numerical results, all the results are intentionally presented with a time axis slightly extending to the prestroke regime.

A. Basic Characteristics of the Induced Currents

Typical induced currents at selected heights obtained from the simulations for reasonably good ground-terminated down conductors (i.e., termination resistance $<24\ \Omega$) are given in Fig. 4.

It can be observed that the induced current in the down conductors is oscillatory in nature with many controlling factors. Its basic characteristics are mainly controlled by the height of the down conductor, the rise time of the current, and the velocity of propagation of the stroke current. It will be shown later that the induced current will also be affected by the magnitude of the footing impedance. Of course, the magnitude of the induced current will depend on the distance between the channel and the down conductor.

Simulation results show that the wave shape of the induced currents is found not to be significantly affected by the inclination of the channel with respect to the vertical, detailed wave shape of the stroke current and the cross-sectional dimensions of the down conductor.

The computed spatio-temporal distribution of the induced currents along the down conductor for a stroke current with 1.2-μs time to peak is given in Fig. 5(a). Only for this case, the actual polarity of the induced current has been retained. The induced currents along the down conductor are expected to propagate in either direction. However, only at the ground end, there will be a positive reflection for the current, resulting in its augmentation. The peak magnitude of the net current, as shown in Fig. 4, decreases toward the top. Depending on the distance between the channel and the down conductor as well as the length of the down conductor, the time difference in the instant of maximum induction along the height of the down conductor can be significant or insignificant. However, the current at various heights along the down conductor, irrespective of its height, seems to oscillate in a coherent mode. This is quite evident from Fig. 4(b). In this figure, the induced current along a down conductor, whose height is set to that of the CN Tower, is presented for a stroke in close proximity (120 m). Although the distance and the vertically straight channel geometry

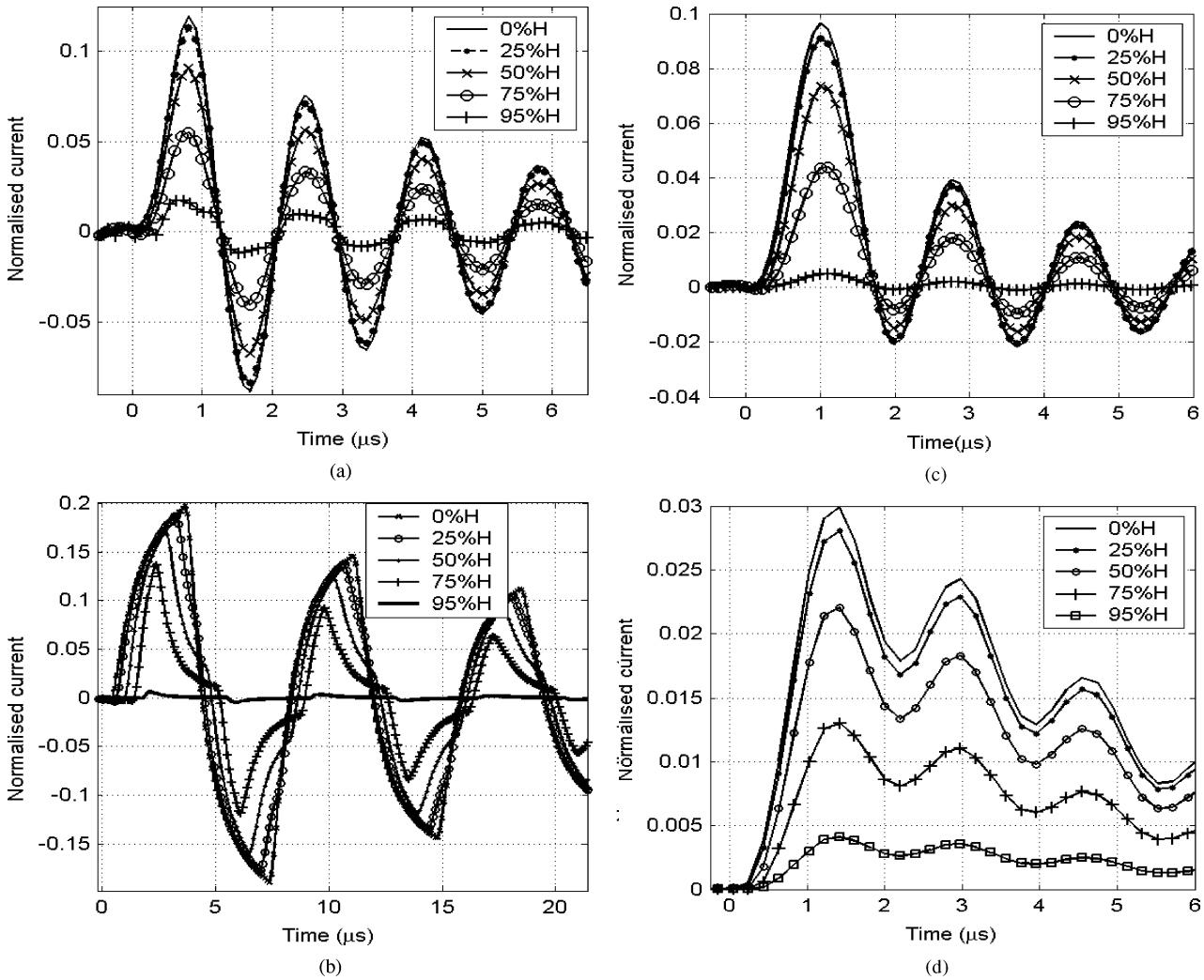

Fig. 4. Induced currents at different heights on various down conductors of radius 3.8 cm. (a) $H = 120$ m; $D = 60$ m; $v = c; t_{\rm p} = 1.2$ μs. (b) $H = 552$ m; $D = 120$ m; $v = c; t_{\rm p} = 1.2$ μs. (c) $H = 120$ m; $D = 60$ m; $v = c/3; t_{\rm p} = 1.2$ μs. (d) $H = 120$ m; $D = 60$ m; $v = c/3; t_{\rm p} = 7.4$ μs.

can be seen to be quite hypothetical, they nevertheless serve the purpose. Due to the close proximity of the channel, the induction along the down conductor occurs with an appreciable time lag. In spite of this, it can be seen that the oscillation of the currents at various heights are in cohesion. The base current is a temporal sum of the downward-propagating current waves that are originated along the down conductor at successive time intervals and the upward reflected waves. Due to this, as can be seen from Fig. 4, the peak of the base current occurs well beyond the instant of maximum induction to the base region.

A further analysis on the oscillatory current reveals that the initial current pulse on the down conductor, which is a reaction to the incident electromagnetic field, causes charging of the down conductor. This aspect is evident from Fig. 5(b) [which corresponds to the induced current given in Fig. 5(a)], wherein the spatio-temporal variation of the charge along the down conductor is given. Once the initial current pulse decays, the influence of the accumulated charge seems to force the current in the opposite direction, which is an attempt toward total neutralization. However, this cycle repeats till the total energy is spent in the resistance heating along the down conductor (which is not fully considered in the present investigation), the ground termination losses, and, of course, the radiation losses. For currents with a slower front, the induced currents shown in Fig. 4(d) will be unipolar to start with, which will be followed by a long tail of opposite polarity. In this case, the portion of current with considerable rate of change spans a time period, which is comparable or even higher than the one-way travel time of the induced current on the down conductor. As a result, considerable induction continues for longer initial time periods, resulting in unipolarity for the initial induced current waveform.

B. Frequency of the Induced Current

Although the induced current exhibits significant oscillations, only for the case of full velocity of propagation and a fast rise time does it possess comparable swing on either side of zero. Furthermore, in other cases, it exhibits dominant first peak, followed by oscillations over a decaying component. These make it difficult to arrive at the frequency of oscillations. For the sake

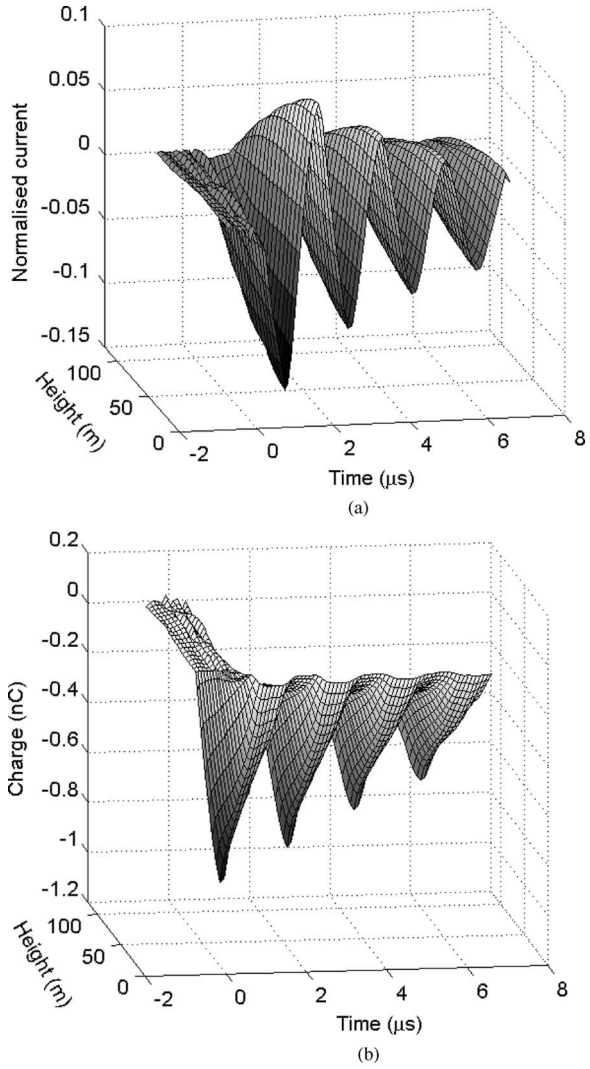

Fig. 5. Spatio-temporal distribution of the induced current and charge. $H = 120$ m; $D = 60$ m; $v = c; t_{\rm p} = 1.2$ μs. (a) Current. (b) Charge.

of evaluation in the present paper, the time period is computed by taking peaks as the reference. This approach will not consider the time taken for the first peak, which will be delayed for the stroke currents with lower values of maximum *di*/*dt* and the lower velocity of propagation.

The frequency of the induced current seems to be determined mostly by the height of the down conductor. It is approximately on the lower side of $f = c/4H$, where H is the height of the down conductor. It is reasonably insensitive to its separation with respect to the channel, the velocity of the current propagation along the channel, the channel inclination, the rise time of the current, and the shape of the current front.

C. Peak Amplitude of the Induced Current

The amplitude of the current is highest near the base, which gradually decreases to zero toward the top. For the simplicity of further discussions, only the maximum peak of the base current is considered. In the following sections, the influence of various channel/stroke current parameters on the base current is considered, which will be followed by the parameters pertaining to the down conductor.

1) Rate of Rise of Stroke Current: Magnitude of induction is clearly dependent on the rate of rise of the stroke current near the ground end of the channel. For any specified value of either the average or the maximum *di*/*dt*, there are innumerable possible currents. For a specified wave shape, the amplitude forms an independent variable, thereby producing the above-mentioned scenario. As mentioned in the beginning of this section, the relation between the induced and the stroke current for a given wave shape and problem geometry is linear. Therefore, the amplitude of the stroke current waveform should not be taken as a variable. Instead, the peak value can be fixed to unity and the dependency between the rate of rise and the magnitude of induction can then be studied. This will facilitate a clear description of the underlying phenomena. With the normalized current, the rate of rise measured between 30% and 90% would be higher than 6, 1, and 0.2 A/μs, respectively, for 5%, 50%, and 95% of subsequent strokes and higher than 0.4, 0.158, and 0.06 A/μs, respectively, for 5%, 50%, and 95% of the first strokes [16].

The lightning current wave shape is a stochastic variable. The stroke current wave shape, as well as the average and the maximum *di*/*dt*, varies from stroke to stroke. Therefore, in order to have a basis for the analysis of the practical data, it becomes necessary to ascertain whether it is the current waveform close to the point of maximum *di*/*dt* or the average rate of rise across major portion of the wavefront that is critical.

In order to answer the first question, a double exponential waveform is first employed. Simulations are carried out for three different wavefronts, i.e., full waveform, waveform clamped at 50%, and waveform clamped at 25%. The maximum value of *di*/*dt* for the double exponential waveform occurs near the origin, and therefore, all three waveforms will have the same maximum *di*/*dt*. Simulations are carried out for different down conductor heights, separations, and *di*/*dt* values. Sample results for the down conductors of height 120 m are presented in Fig. 6. For the waveforms with slower fronts, the instant of clamping occurs much later as compared to the waveforms with faster fronts. In other words, as measured with respect to the one-way travel time of the current along the down conductor, for slower front currents, clamped waveform and the original one will be closer to each other for longer time durations. The consequence of this is evident from Fig. 6. The induction due to full and clamped waveforms differs from each other only for currents with faster fronts. This observation indicates that the travel time along the down conductor might decide the most influential region around the maximum *di*/*dt* of the stroke current. For verifying this, instead of clamping at a fixed magnitude, waveforms are clamped at a time instant, which is selected in terms of one-way travel time (H/c) along the down conductor. The simulation results indicate that the wavefront spanning around $1.5H/c$ is the most influential region of the current. The results corresponding to this are also shown in Fig. 6.

For the same value of maximum *di*/*dt*, stroke currents can have different average *di*/*dt* along their front. For example, with the first strokes, the maximum *di*/*dt* occurs near the upper half of the wavefront, and the average rate of rise measured around

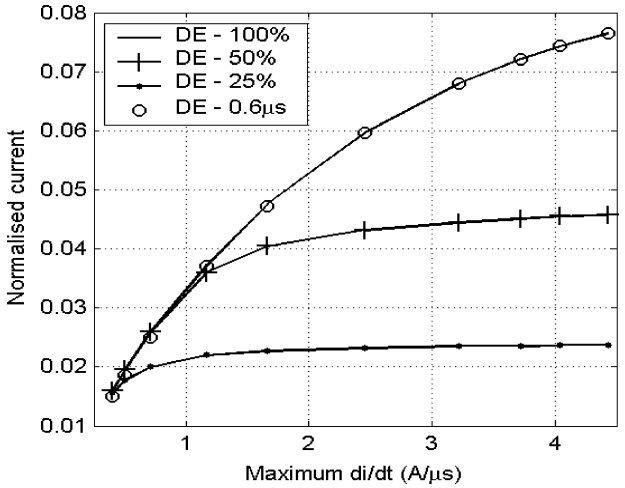

Fig. 6. Peak value of the induced base current for different stroke current waveforms. $H = 120$ m; $D = 120$ m; $v = c$. DE-100%: full double exponential. DE-50%: double exponential clamped at 50%. DE-25%: double exponential clamped at 25%. DE-0.6 μs: double exponential clamped to its value at 1.5 H/c.

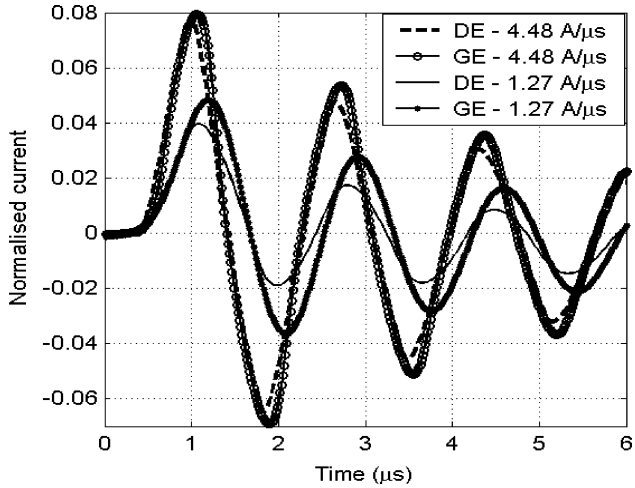

Fig. 7. Induced base currents for stroke currents with two different maximum *di*/*dt*. $H = 120$ m; $D = 120$ m; $v = c$. DE: double exponential. GE: Gaussian-like front exponential tail.

the region of maximum *di*/*dt* would be higher as compared to that with the double exponential. In order to scrutinize this, simulations were carried out with a new type of waveform, which possesses a higher resemblance to the stroke current.

In lightning statistics, the rise time between 10% and 90% and 30% and 90% are specified [16]. Such data are more advantageous as they are stated independent of the stroke current. Although the two data could be independent, they can be imposed on the same stroke current waveform. Then, the resulting waveform can be treated as a representative waveform. With this perspective, a modified waveform with a Gaussian-like front and an exponential tail is deduced. The tail portion, starting from the peak value, is the same as the double exponential waveform and, therefore, will not be discussed further. As two constraints are to be enforced on the front of the current, a two-parameter function is required, which should be concave upward at the beginning. Considering all these, we arrive at the following function:

$$I(t) = \exp\left(-\frac{|t|^{\alpha}}{\beta}\right).$$

The tail portion following the peak is set to that of the double exponential function. In the above expression, the time t must be specified in microseconds. By performing curve fitting over the specified values of the above rise times for both the first and the subsequent negative strokes, the corresponding values for α and β are deduced. The values of these parameters employed for the present work can be found in the list below (which corresponds to time specified in microseconds).

$$\alpha = [1.0010 \quad 1.1290 \quad 1.2790 \quad 1.4360 \quad 1.5990 \quad 1.7690 \quad 1.9930 \quad 2.4730 \quad 2.9910 \quad 3.5340 \quad 4.0800 \quad 4.8430 \quad 5.9820 \quad 5.7110 \quad 4.1380 \quad 3.0810 \quad 2.4830 \quad 1.9240 \quad 1.7850 \quad 1.8210 \quad 2.4180]$$

$$\beta = [0.0909 \quad 0.0848 \quad 0.0789 \quad 0.0750 \quad 0.0729 \quad 0.0725 \quad 0.0745 \quad 0.0887 \quad 0.1256 \quad 0.2116 \quad 0.4164 \quad 1.4017 \quad 26.3026 \quad 63.8869 \quad 25.0559 \quad 10.8932 \quad 7.1687 \quad 5.5405 \quad 5.7619 \quad 10.1229 \quad 61.7731].$$

The rise time between 10% and 90% corresponding to the above values is given by $t_r(\mu s) = [0.200 \quad 0.220 \quad 0.240 \quad 0.260 \quad 0.280 \quad 0.300 \quad 0.325 \quad 0.375 \quad 0.425 \quad 0.475 \quad 0.525 \quad 0.600 \quad 0.800 \quad 1.000 \quad 1.400 \quad 1.800 \quad 2.200 \quad 3.00 \quad 3.500 \quad 4.60 \quad 5.60]$.

The respective rise time (in microseconds) between 30% and 90% can be found by the equation

$$0.0189\, t_{\mathrm{r}}^3 - 0.1558\, t_{\mathrm{r}}^2 + 0.9733\, t_{\mathrm{r}} - 0.0886.$$

For very slow wavefronts, the peak region as given by the above is overly flat. However, the induction due to very slow front is not significant, and therefore, the above deficiency can be ignored. The above waveform has its maximum *di*/*dt* at the upper portion of the front, and its average steepness is higher than the double exponential wave.

Simulations are carried out for different values of rise times. It is found that, in general, for a given value of maximum *di*/*dt*, the magnitude of the induced current is relatively lower for the double exponential wave. This difference, as shown in Fig. 7, is not considerable for fast fronted stroke currents and can reach 10%–20% for slower fronts. This can be attributed to lower values of average rate of rise (measured around the steep portion) of the double exponential waveform.

Similar to the double exponential case, studies were conducted to ascertain the region around the maximum *di*/*dt* point, which could significantly influence the determination of the magnitude of the induction. From the original waveform, only the region symmetrically cut around the point of maximum *di*/*dt* is selected and taken as the channel current. Results show that the conclusion made earlier, that the region around maximum

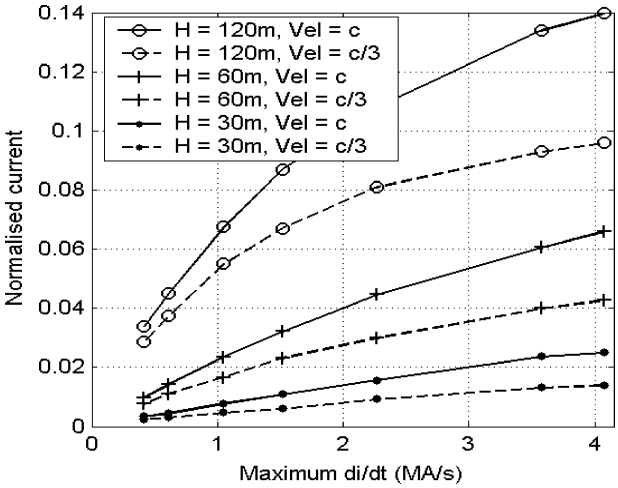

Fig. 8. Dependency of the peak value of the base current on maximum *di*/*dt* of the channel current. $D = 60$ m.

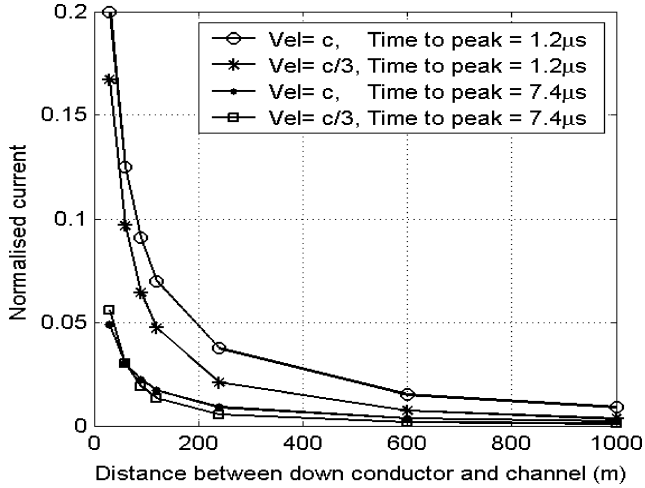

Fig. 9. Dependency of the peak value of the base current on the gap. $H = 120$ m.

di/*dt* spanning around $1.5H/c$, is most influential in governing the induction.

With the above observations, further investigations are carried out to ascertain the dependency of the peak amplitude of the induced currents on the maximum *di*/*dt* of the normalized stroke current. The simulation results with double exponential function for the stroke current shown in Fig. 8 indicate that for a given down conductor height, the relation seems to be linear for rise times in the range of subsequent return strokes. However, for slower pulses like the typical first strokes, this dependency seems to be higher, and the peak magnitude of the induced current decreases faster with respect to a given change in the maximum *di*/*dt*.

2) Velocity of Propagation of the Stroke Current: The expressions for the field produced by the channel are available in the literature [14]. They involve spatial integrals, which contain the spatio-temporal current in the integrand. The value of the integral is dependent on the distance up to which the stroke current has propagated. This in turn depends on the location of the observation point and time. For a given time, it can be seen that for lower velocities of propagation, relatively lower lengths of the channel will carry the stroke current, and therefore, the resulting integral will also be lower. This aspect becomes evident when the peak amplitudes of the induced currents are plotted for different maximum *di*/*dt* and velocity of propagation of the current. Fig. 8 shows the typical results for three different heights with a fixed separation of 60 m. The dependency on the velocity can be seen to diminish for slower current pulses. In these cases, due to their larger time duration, the rising portion of current containing maximum *di*/*dt* spans the larger length of the channel. Moreover, the duration of considerable induction to the down conductor also increases. Consequently, the influence of velocity diminishes.

Simulations carried out for down conductors of height 30 and 60 m with a gap of 50% of their heights reveal a lower dependency on the velocity than that indicated in Fig. 8. In these cases, due to a small separation, the portion of the channel closest to the given portion of the down conductor causes appreciably more induction than the remaining portion of the channel. As a result, dependency on the velocity diminishes.

3) Distance Between the Channel and the Down Conductor: As can be expected, the amplitude of the induced current depends on the radial distance between the down conductor and the channel. However, the exact dependency is not amicable to simple calculations as both the source and the down conductor are spatially distributed with the ground also being in action. The simulation results, which are given in Fig. 9, indicate that the dependency of the induced currents on the separation is slower than 1/distance. Here, the fast and the slow fronts correspond to maximum *di*/*dt* of 3.6 and 0.43 MA/s, respectively. This dependency seems to be similar for both full and reduced velocity of the return stroke currents. The larger separations have been considered only for demonstration and not for any actual quantification. This restriction is due to the assumption of a perfect ground. However, it should be noted that as the induced currents for strokes terminating at larger distances will be of much smaller strength, analysis for them is not necessary.

4) Inclination of the Channel: In reality, the locus of the channel will be quite complicated and will never be perfectly vertical. However, the actual locus is a stochastic variable and cannot be comprehended at this stage. In view of this, most of this preliminary study is carried out with a vertical channel. Therefore, it becomes necessary to ascertain the possible influence of the channel inclination on the induced currents. For the analysis, a straight channel with different inclinations are considered. As shown in Fig. 3(b), only the inclinations going away from the down conductor are considered. Simulation results given in Table I for different gaps and inclinations reveal that the magnitude of the induced currents decreases with inclination to the vertical. In the above, both the channel and the down conductor are in the same plane. Now, if the channel inclination perpendicular to the above is considered, then the induction is found to be higher but still lower than that for a vertical channel.

TABLE I
NORMALIZED INDUCED BASE CURRENTS FOR DIFFERENT CHANNEL INCLINATIONS (VELOCITY = c, TIME TO PEAK = 1.2 μS)

Inclination	Separation distance from the channel		
	60 m	120 m	240 m
0°	12.7×10^{-2}	7.1×10^{-2}	3.8×10^{-2}
10°	10.1×10^{-2}	5.9×10^{-2}	3×10^{-2}
22.5°	8×10^{-2}	4.6×10^{-2}	2.6×10^{-2}
45°	5×10^{-2}	2.9×10^{-2}	1.6×10^{-2}

Further, at least the portion forming the last jump, which is assumed in this section to be directly linked to the ground, cannot be fully inclined. Therefore, it would be more appropriate to consider the last section of the channel to be closer to the vertical and the remaining portion to be inclined. Even under this supposition, the length of the last section of the channel is not a fixed entity, and in view of this, a length lower than the height of the down conductor, which is followed by a length equal to as well as greater than the down conductor height, is considered. The simulation results show that if the last section, which is assumed to be vertical, is of a length equal to or greater than that of the down conductor, then the magnitude of the induced current is the same as that with a fully vertical channel (irrespective of the inclination of the second section of the channel). However, if it is lower, then the induced current will also be of a lower magnitude.

This shows that the activities in the last section of the channel linking to the ground are more influential than the remaining sections. Implicitly, this indicates that the branching originating from an elevated point on the channel, the actual geometry of the channel, which is rather complicated to consider, and the decay of velocity and current along the channel [17] are all not very influential in determining the induced currents. Therefore, from the point of view of the above-mentioned entities, the model for the channel employed in the present paper seems to be adequate. However, the same cannot be generalized with regard to the elevated attachment point.

5) Radius of the Down Conductor: The radius of the down conductor does not seem to have any strong influence on the amplitude of the induced currents. A study with down conductor heights of 30–120 m and radius between 1 mm and 60 cm reveals that for a large change in radius of the order of 600, the corresponding change in the peak of the induced currents is well within a factor of 2.25–3. The lowest radius selected for the study is, of course, not very realistic but simply employed for demonstrating the fact. Even if a tower of base 14 m $\times$ 14 m is taken as the down conductor, the increase in the peak current is well within a factor of four. The detailed dimension of the tower is given in [12]. By considering the down conductor as a receiving antenna (as suggested by the referees of this paper), the dependency on the radius can be directly analyzed. The impedance of an isolated antenna when used for receiving is the same as that when used for transmitting. The average characteristic impedance [18] of the down conductor as a monopole antenna is then given by

$$60\left(\log\frac{2H}{r}-1\right).$$

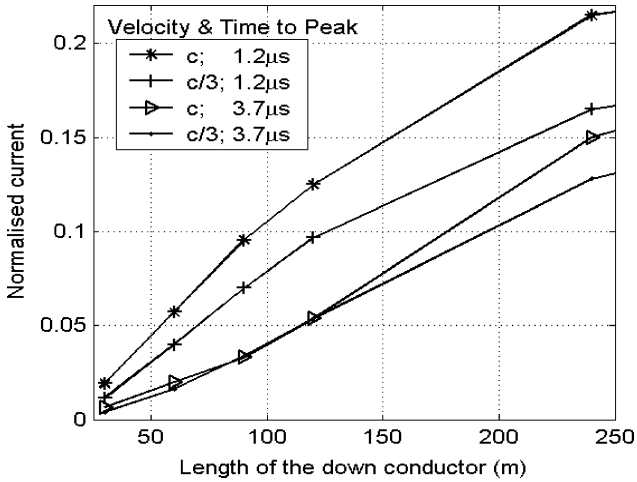

Fig. 10. Dependency of the peak value of the induced current on the length of the down conductor. $D = 60$ m.

The computed currents for cylindrical down conductors of different radii agree well with the scaling ratio given by the above function. In other words, the increase in current with the radius of the down conductor seems to be governed by the logarithmic function.

6) Length of the Down Conductor: The base current is a temporal sum of the downward-propagating current waves, which are originated along the down conductor at successive time intervals and the upward reflected waves. Due to this, as can be seen in Fig. 4, the peak of the base current occurs well beyond the instant of maximum induction to the base region. Therefore, the magnitude of the base current can be expected to increase with the height of the down conductor. However, as the height of the down conductor increases, the time delay in the arrival of the induced currents at elevated points becomes appreciable, and as a result, the addition of the current at the base gets smeared out in time. Consequently, the magnitude of the base current does not increase proportionately with the height of the down conductor. The peak amplitude of the base current for different down conductor lengths are given in Fig. 10. In this case, as can be expected, the radius of the down conductor and the gap between it and the channel were held similarly.

D. Wave Shape of the Induced Current

The shape of the induced current depends on several factors, such as height of the down conductor and the height at which the current is measured, the maximum di/dt of the return stroke current, the velocity of propagation of the return stroke current, the ground termination resistance (and inductance), the distance between the channel and the down conductor, and the cross-sectional dimensions of the down conductor. (It may be noted here that this section will deal only with the shape and not with the magnitudes.) Fig. 4 strongly supports the above statement.

It can be observed that the induced current has significant oscillatory components. For fast-rising return stroke currents, the induced current seems to possess comparable negative swings,

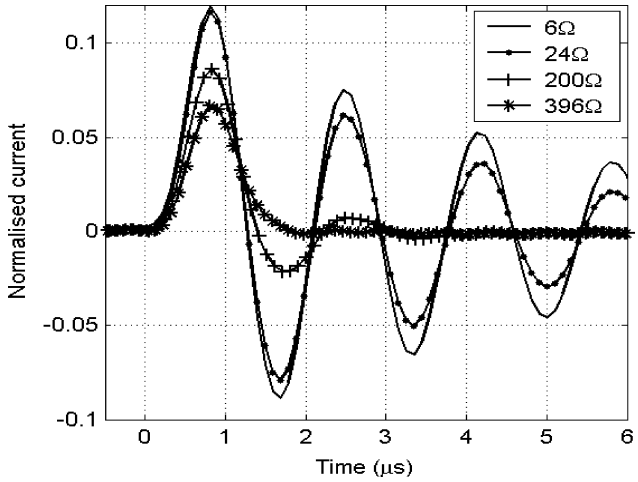

Fig. 11. Base current in the 120-m-tall down conductor for different footing resistances. $D = 60$ m; $v = c; t_{\rm p} = 1.2$ μs.

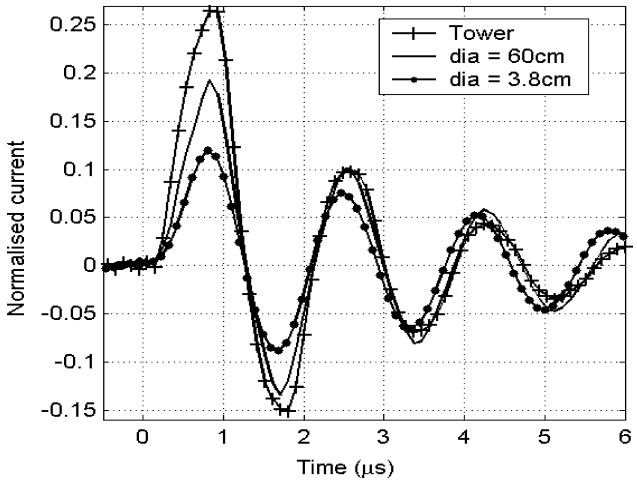

Fig. 12. Base currents for the 120-m-tall down conductor for different radii. $D = 60$ m; $v = c; t_{\rm p} = 1.2$ μs.

whereas for slower pulses and reduced velocity of propagation of return stroke currents, the induced current is mostly unipolar at the beginning. After this stage, an opposite polarity current with relatively slow decay rate in the range of tens of microsecond (for the 120-m-long down conductor) appears. The current magnitude at this stage and that in subsequent oscillations is found to be quite low.

The velocity of propagation of the stroke current and the separation distance seem to influence the wave shape of the induced current. Fig. 4 depicts this dependency. The wave shape is basically altered by the time lag in the induction of the current in each section of the down conductor, which can be directly related to the distance between the channel and the down conductor and the stroke current distribution along the channel. With slower current pulses and lower velocity of propagation, induction to the down conductor seems to be smeared out in time, resulting in prolonged time to first peak, as well as holding the current to one polarity for the first few microseconds.

Duration of the induced currents or the decay rate is dependent on the footing resistance (Fig. 11). The first two values, i.e., 6 and 24 Ω, correspond to the upper limit for the impedances evaluated for two of the practical systems, whereas the last two values of the resistance are selected for the illustration of the phenomena. Here, it may be recalled that the actual impedance offered by the down conductor to the lightning current is not constant for all time (or frequency) regimes. However, for comparison, it has been customary to employ a step (or step like) surge and compute the value for the impedance as the ratio of the voltage to the current just at the time of arrival of the first reflection from the ground end [7], [12]. For footing resistances of value much less than the "surge impedance" of the down conductor (typically 150–400 Ω), the actual value of the resistance possesses insignificant influence on the amplitude of the dominant peak. However, the value of the footing resistance, even when it is smaller than the surge impedance of the down conductor, is highly influential in dictating the current decay rate. As mentioned earlier, roughly half of the current induced at various heights, as well as the current wave reflected at the top open end, are directed toward the ground. The reflected wave from the ground end, as it propagates, augments the current. Now, by applying the classical transmission line wave theory, of course only as a crude approximation, it can be seen that as long as the footing impedance is much smaller than the "surge impedance" of the down conductor, irrespective of the value of the footing resistance, the reflection coefficient at the ground end remains the same. Consequently, the first peak of the base current does not get affected. However, the losses in the system will be dependent on the footing resistance, and hence, the decay rate will get affected. With footing resistance close to the "surge impedance," not only does the magnitude of the first peak decrease, but the subsequent current also decays down to negligibly small values. Perhaps, in practical situations, wherein the grounding system has been affected by aging and chemical degradation in the soil, the effective impedance for smaller current can be quite high. However, as soon as the current exceeds a certain value, the resulting soil gradient can reach the breakdown gradient of the soil (2–5 kV/cm) [19], resulting in effectively low impedance. The ramifications of this can be deduced from the above discussion.

The cross section of the down conductor apart from determining the magnitude of the induced currents is also found to influence the current decay rate. It is evident from Fig. 12 that a higher cross section will result in a faster decay of current, which for lower frequency regimes can be approximately linked to the lowering of the inductance and, hence, the time constant. The trend is very similar for the induced current due to slower stroke currents. Of course, in that case, the current in the beginning can be quite unidirectional. The result for the induced current in the tower is also shown in Fig. 12, and it can be seen to follow the same trend. The basic dimensions of the tower are taken from [12]. In the case of the tower, the induced current in the legs are not the same. The current in the legs on the illuminated face is found to be higher than that of the rear side.

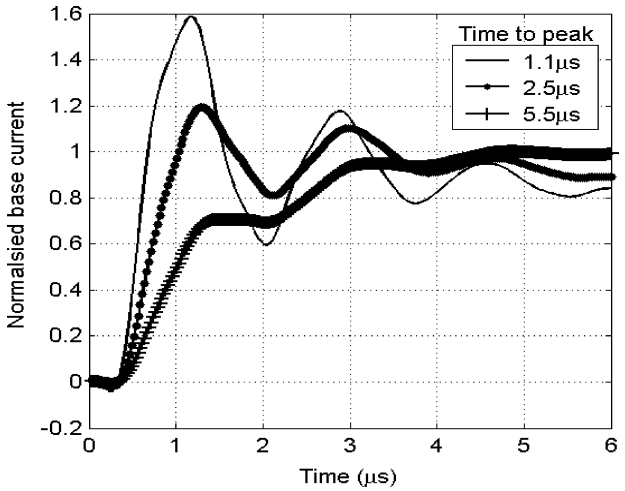

Fig. 13. Base current on the 120-m-tall down conductor for a direct hit.

IV. Comparison With Current During a Direct Hit

A comparison between the induced base currents with those during a direct hit would be of considerable practical interest. Obviously, on the whole, the currents during a direct hit would be of much larger magnitude; however, this can serve only as a supporting evidence rather than a categorizing entity. For a comparison, the computed base currents during a direct hit are given in Fig. 13. Typically, irrespective of the time to peak, all the waveforms merge into the incident stroke current (which is assumed to be unaffected by the presence of the down conductor). The other salient features of the base currents during a direct hit, as compared to the induced currents, are a lower magnitude of oscillation, a much longer duration, a unipolar waveform, and the decay of oscillation into a smooth waveform.

V. Strike to an ESO

A strike to an ESO needs special attention as the resulting traveling current wave suffering successive reflections at either ends of the ESO is shown to modify the field [20], [21]. Therefore, several questions arise on the nature as well as the magnitude of the induction into the down conductor.

A few simulations are carried out with ESO modeled as a vertical cylindrical conductor. Both the down conductor and the ESO are terminated at the ground with a resistance of 6 Ω. Some typical results for a down conductor of 120 m length are given in Fig. 14. In Fig. 14(a), a strike to the ground and strike to the ESO of heights 60 and 240 m have been considered. In Fig. 14(b), a strike to the ESO of 120 m height is considered with two different times to peak for the stroke current. The characteristics of the induced currents are also found to depend on the distance between the ESO and the down conductor. As shown in Fig. 14(c), for higher separation distances, the peak magnitude of the induced currents during a strike to the ESO is found to be higher than that for a strike to the ground.

The field produced by the current waves in the ESO is found to significantly alter the shape of the induced down conductor currents. When the height of the ESO becomes different from that of the down conductor, the induction due to the current

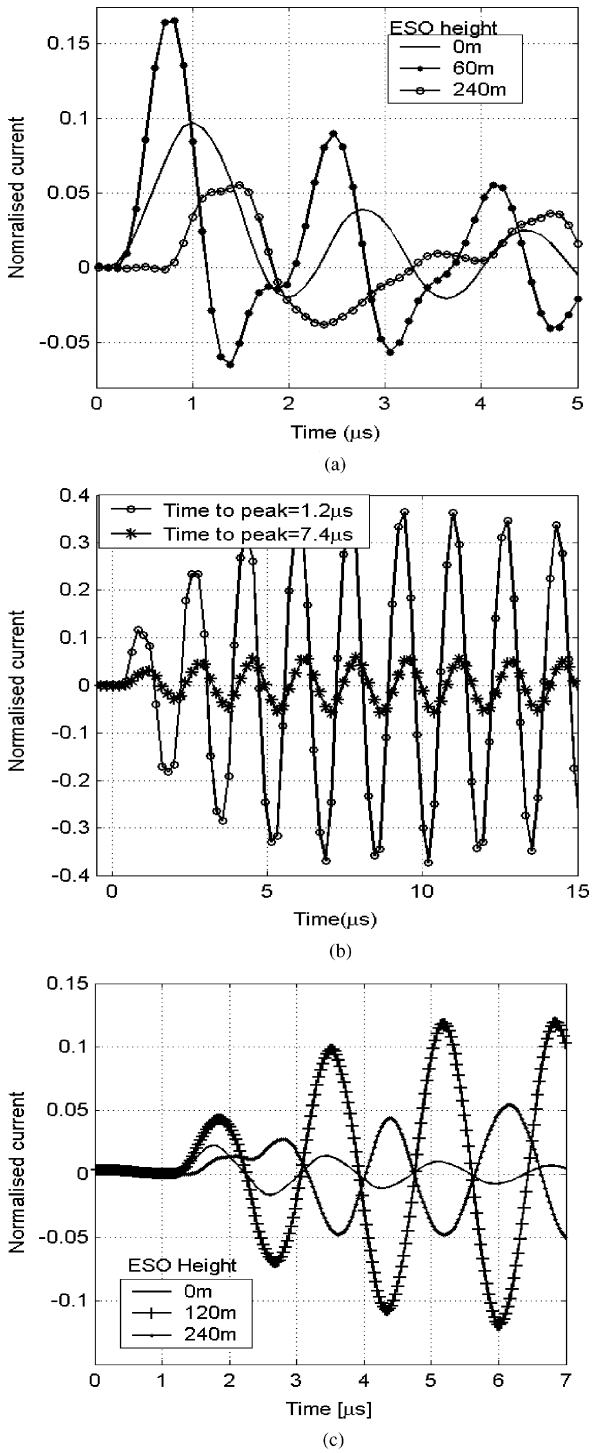

Fig. 14. Induced base current on the 120-m-tall down conductor. (a) Strike to the ESOs of different heights. $D = 60$ m; $v = c/3; t_{\rm p} = 1.2$ μs. (b) Strokes with different times to peak. $D = 60$ m; $v = c/3$; height of the ESO $= 120$ m. (c) Strike to the ESOs of different heights. $D = 360$ m; $v = c/3; t_{\rm p} = 1.2$ μs.

waves along the ESO will be asynchronous with the oscillations in the induced down conductor currents. This, as shown in Fig. 14(a), results in the distortion of the induced current waveforms. Depending on the position of the down conductor and the time instant of the observation, the continued induction due to the current waves along the ESO could be aiding or opposing.

As a result, at any given instant, current at any point on the ESO could be enhanced or reduced. Further, the base current, which is a sum of all the downward moving currents along the ESO and the positively reflected waves, assumes magnitudes that are dependent on the instant of arrival of the downward currents. The consequence of the same is clearly depicted in the spatial distribution of current along the ESO. In the case of a strike to an ESO of height 60 m at a distance of 60 m, the induced base current is enhanced for the initial time period, whereas the current in the upper half of the down conductor is relatively reduced. However, in the case of strike to an ESO of height 240 m, the base current is reduced, whereas, relatively, the average current in the down conductor is enhanced.

When the height of the ESO matches that of the down conductor, the field due to successively reflected current waves along the ESO aid the induced current in the down conductor, resulting in a buildup of the induced currents. Consequently, instead of the first peak, depending on the footing resistance, the subsequent peak assumes the maximum value.

The induced currents during strike to an ESO need a detailed investigation, which is left for a future work. The findings of Baba and Rakov [21] would be of considerable interest in this regard.

VI. Summary and Conclusion

Cloud-to-ground lightning in the vicinity induces significant currents in tall down conductors and other conducting structures. Knowledge of the characteristics of such induced currents is required for the scrutinization of the recorded lightning current data on instrumented towers. This paper has attempted a basic theoretical study of the characteristics of induced currents on simple vertical down conductors during a nearby strike. Electromagnetic model has been employed for the study. The numerical model has been validated with experimental results obtained in the laboratory.

The basic characteristics of the lightning-induced currents and the influence of various parameters like the distance between the down conductor and the channel, the radius of the down conductor, the footing resistance of the down conductor, the channel geometry, the wave shape of the current, the velocity of the return stroke current, etc., on the same have been studied. Some of the main results are summarized here.

The nature of the induced current is highly dependent on the rate of rise as well as the velocity of propagation of the stroke current. The magnitude and, to some extent, the wave shape of the induced current is found to depend on the average as well as maximum di/dt of the stroke current. For a given wave shape, the magnitude of the induced current increases with the rate of rise of the wavefront; however, a saturating trend will onset at some point.

The height of the down conductor mainly governs the frequency of the oscillatory component of the induced current. The magnitude of the induced current is found to increase with the height of the down conductor, which exhibits a saturating trend at a certain height. The dependency of the induced current on the radius of the down conductor seems to be logarithmic (which is in accordance with the AT).

During a strike to an ESO, the height of the ESO is found to have a significant influence. When its height matches that of the down conductor, significant amplification of the induced current is seen.

In this paper, the upward connecting leader activity from the down conductor and the charge induced on the down conductor by the leader phase have been neglected. These need to be addressed and the results compared against the relevant field data.

Acknowledgment

The authors would like to acknowledge valuable suggestions made by the referees in improving the presentation of this paper.

References

[1] A. Borghetti, J. A. Gutierrez, C. A. Nucci, M. Paolone, E. Petrache, and F. Rachidi, "Lightning-induced voltages on complex distribution systems: Models, advanced software tools and experimental validation," *J. Electrost.*, vol. 60, pp. 163–174, Mar. 2004.

[2] M. G. Sorwar, H. Ahmad, and M. M. Ali, "Analysis of transients in overhead telecommunication subscriber line due to nearby lightning return stroke," in *Proc. IEEE Int. Symp. Electromagn. Compat.,* Aug. 24–28, 1998, vol. 2, pp. 1083–1088.

[3] E. Petrache, F. Rachidi, M. Paolone, C. A. Nucci, V. A. Rakov, and M. A. Uman, "Lightning induced disturbances in buried cables—Part I: Theory," *IEEE Trans. Electromagn. Compat.*, vol. 47, no. 3, pp. 498–508, Aug. 2005.

[4] M. Paolone, E. Petrache, F. Rachidi, C. A. Nucci, V. A. Rakov, M. A. Uman, D. Jordan, K. Rambo, J. Jerauld, M. Nyffeler, and J. Schoene, "Lightning induced disturbances in buried cables—Part II: Experiment and model validation," *IEEE Trans. Electromagn. Compat.*, vol. 47, no. 3, pp. 509–520, Aug. 2005.

[5] S. Miyazaki and M. Ishii, "Lightning current distribution inside of directly hit building," in *Proc. XIV Int. Symp. High Voltage Eng.*, Beijing, China, Aug. 25–29, 2005, vol. A, pp. A-26/1–A-26/5.

[6] J. Kato, H. Kawano, T. Tominaga, and S. Kuramoto, "Investigation of lightning surge current induced in reinforced concrete buildings by direct strikes," in *Proc. IEEE Int. Symp. Electromagn. Compat.*, Aug. 2001, vol. 2, pp. 1009–1014.

[7] Y. Baba and M. Ishi, "Numerical electromagnetic field analysis of lightning current in tall structures," *IEEE Trans. Power Del.*, vol. 16, no. 2, pp. 324–328, Apr. 2001.

[8] B. Kordi, R. Moini, W. Janischewskyj, A. M. Hussein, V. O. Shostak, and V. A. Rakov, "Application of the antenna theory model to a tall tower struck by lightning," *J. Geophys. Res.*, vol. 108, no. D17, 4542, pp. ACL7/1–ACL7/9, 2003.

[9] Y. Baba and M. Ishi, "Characteristics of electromagnetic return-stroke models," *IEEE Trans. Electromagn. Compat.*, vol. 45, no. 1, pp. 129–134, Feb. 2003.

[10] G. J. Burke and A. J. Poggio, "Numerical electromagnetic code (NEC)-method of moments, Part I & III," Naval Ocean Syst. Center, San Diego, CA, Tech. Rep. 116, 1980.

[11] R. Moini, B. Kordi, G. Z. Rafi, and V. A. Rakov, "A new lightning return stroke current model based on antenna theory," *J. Geophys. Res.*, vol. 105, no. D24, pp. 29 693–29 702, 2000.

[12] U. Kumar and P. Kumar, "Investigations on the voltages and currents in lightning protection schemes involving single tower," *IEEE Trans. Electromagn. Compat.*, vol. 47, no. 3, pp. 543–551, Aug. 2005.

[13] R. H. Golde, "The earth flash," in *Lightning*, vol. 1, R. H. Golde, Ed. New York: Academic, 1977.

[14] C. A. Nucci, G. Diendorfer, M. A. Uman, F. Rachidi, M. Ianoz, and C Mazzetti, "Lightning return stroke current models with specified channel-base current: A review and comparison," *J. Geophys. Res.*, vol. 95, no. D12, pp. 20 395–20 408, Nov. 1990.

[15] V. Shivanand, "Preliminary studies on the characterisation of the induced current in simple down conductors due to a nearby lightning strike," M.E. thesis, Dept. High Voltage Eng., Indian Inst. Sci., Bangalore, 2005.

[16] International Electrotechnical Commission (IEC) 61024-1, "Protection of structures against lightning—Part I: General principles," Geneva, Switzerland, 1993-03.

[17] V. Cooray, "The lightning flash," *Inst. Elect. Eng. Power Ser.*, vol. 34, 2003.
[18] E. C. Jordan and K. G. Balmain, "Electromagnetic waves and radiating systems," *Prentice-Hall Elect. Eng. Ser.*, 2nd ed., 27th Indian Reprint, 1988.
[19] V. Cooray, M. Zitnik, M. Manyahi, R. Montano, M. Rahman, and Y. Liu, "Physical model of surge–current characteristics of buried vertical rods in the presence of soil ionisation," *J. Electrostat.*, vol. 60, pp. 193–202, Mar. 2004.
[20] V. A. Rakov, "Transient response of a tall object to lightning," *IEEE Trans. Electromagn. Compat.*, vol. 43, no. 4, pp. 654–661, Nov. 2001.
[21] Y. Baba and V. A. Rakov, "Lightning electromagnetic environment in the presence of a tall grounded strike object," *J. Geophys. Res.*, vol. 110, pp. D09108/1–D09108/18, May 2005.

Udaya Kumar received the B.E. degree in electrical engineering from Bangalore University, Bangalore, India, in 1989 and the M.E. and Ph.D. degrees from the Department of High Voltage Engineering, Indian Institute of Science, Bangalore, in 1991 and 1997, respectively.

He is currently an Assistant Professor in the Department of High Voltage Engineering at the Indian Institute of Science. His current research interests include modeling of lightning, analysis and design of lightning protection systems, and electromagnetic field analysis pertaining to insulation and lightning.

Vishwanath Hegde received the B.E. degree from the University of Mysore, Mysore, India, in 1986 and the M.E. degree from the Indian Institute of Science, Bangalore, India, in 1991, both in electrical engineering. He is currently working toward the Ph.D. degree at the Indian Institute of Science.

His current research interests include lightning, electromagnetic field analysis pertaining to insulation, and lightning protection.

Vinoda Shivanand received the B.E. degree in electrical engineering from Gulbarga University, Gulbarga, India, in 1997. She is currently working toward the Master's degree at the Indian Institute of Science, Bangalore, India.

Her current research interests include lightning protection.